Determining the Most Influential Parameters on the Performance of a Railway Transition Zone

By:
Jasper Blokdijk

Thesis committee:
Dr. V.L. Markine
Prof. dr. ir. R.P.B.J. Dollevoet

A thesis presented for the degree of
Bachelor of Science

Department of Civil Engineering
Delft University of Technology
July 9, 2024

Preface

This bachelor's thesis will be about determining the most critical parameters of a railway transition zone while taking uncertainties into account. This thesis is written for the sector railway engineering within the structural engineering sector. This thesis is written as a final requirement for a bachelor's degree in Civil Engineering at TU Delft.

This thesis is written for people that are interested in stochastic sampling techniques and railway engineering. To understand this thesis, some knowledge is expected in these fields of research. However, most concepts will be explained.

I would like to thank my supervisors, Dr. V.L. Markine and Prof. dr. ir. R.P.B.J. Dollevoet for their guidance while writing this thesis.

Jasper Blokdijk
Delft, July 9, 2024

Summary

Railway transition zones represent a significant challenge due to abrupt variations in substructure properties, leading to differences in vertical strain. These differences cause the wheel-rail dynamic interaction to get excited, which can cause passenger discomfort, track deterioration, and derailment. Consequently, proactive design strategies are crucial to mitigate these stresses. In previous research, an optimal geometry of railway sleepers was designed, however it was assumed that every sleeper would have the same geometry. This renders the design to be susceptible to inherent uncertainties. To address this limitation, a new design should be made incorporating uncertainties. However, railways involve numerous parameters influencing performance. Employing all parameters within an optimization framework is computationally not feasible. Therefore, this thesis aims to identify the most influential design variables within a railway transition zone. This leads in the following research question:

How can the most influential design variables on the performance of a railway transition zone be determined using a static model while taking uncertainties into account?

In this research, the design variables have been limited to only railway sleepers. To answer this question, a comprehensive review on how uncertainty is implemented into designs was done. Leveraging this knowledge, optimized Latin Hypercube Sampling (OLHS) was employed to generate samples defining the length and width of each sleeper within the transition zone. These samples were then used as input variables within a static Ansys model, modified to mimic dynamic factors. This model subsequently calculates the stress and settlement in the ballast and soil layer for several locations across the transition zone. This process is repeated for ten different samples created with OLHS. The location exhibiting the highest settlement and stress for each sample was identified, resulting in a dataset for comparison between the samples with the most favorable and least favorable performance.

One pattern that can be seen in the results is that higher stresses occur when there is a higher disparity between adjacent railway sleepers. This may be the cause of differences in bearing surface area, where longer sleepers spread the load from the rails over a larger area than shorter sleepers. This causes uneven settlement, and consequently higher stress concentrations. If this hypothesis holds true, incorporating gradual transitions in sleeper length throughout the transition zone becomes a critical design consideration for future optimization efforts. However, further research is warranted to definitively validate this observation.

Table of Contents

1 Introduction

Transition zones are a well-known challenge in the railway industry due to the sudden change in substructure characteristics, which causes differences in vertical strain. These variations can result in ”hanging sleepers”, which cause the wheel-rail dynamic to get excited. This accelerates track deterioration, causes discomfort for passengers, and increases the chance of accidents like derailment.

Currently corrective mitigation techniques like tamping are used to address track deterioration. However, these methods generally result in faster deterioration. To combat this issue, preemptive mitigation measures should be implemented to reduce stresses in the subsoil, which is the primary cause for settlement underneath the track. One effective approach is to optimize the geometry of a transition zone. An optimal design will be able to distribute stresses better, which can enhance track longevity.

Previous research has focused on optimizing the railway sleepers in transition zones. However, here was assumed that all sleepers would have the same geometry. The deterministic nature of this design causes it to be more susceptible to uncertainties. A new optimal design should be made, that takes these uncertainties into account. The design of a railway has a lot of parameters that influence its performance however. Using all of these parameters while optimizing is not feasible due to high computation times. Therefore, only the most influential parameters should be taken into account.

This leads to the research question: ”How can the most influential design variables on the performance of a railway transition zone be determined using a static model while taking uncertainties into account?” Here, design variables will be limited to railway sleeper geometry. This question will be tried to answer using the following sub-questions: ”What are uncertainties and how can they be accounted for during design processes?”, ”How can dynamic factors that influence the railway transition zone be implemented into a static model?” and ”How can the influence of the design variables of the railway transition zone be quantified using a static model?” These questions will be answered using a literature review on the implementation of uncertainties in design, a static Ansys model of a railway transition zone and Python language coding to change parameters and run the model.

Chapter 2 will delve deeper into the problems with current transition zones and will outline the objectives of the report. Chapter 3 will cover the literature review about the implementation of uncertainties into a design. Chapter 4 will explain the Ansys model provided, and the changes made to it to try and simulate dynamic factors. Chapter 5 will discuss the final preparatory steps leading up to the experiment, as well as the methodology of this experiment. Chapter 6 will present the results of this experiment. Chapter 7 will discuss said results and highlight any implications with it. Finally, Chapter 8 will present the conclusions drawn from the research and gives recommendations for possible future research.

2 Problem analysis

In this chapter a description of the problem that will be attempted to solve is given. First, background information about railway sleepers and transition zones will be given. After that, previous research will be looked at and the knowledge gaps within those studies will be pointed out. Finally, the objective of this study will be discussed.

2.1 Problem

Railway tracks can be supported by various constructions, with ballasted and slab tracks being the most prevalent types. Traditionally, ballasted tracks are more commonly utilized due to their lower initial cost. However, in areas where maintenance is expected to be more frequent, such as high-speed railways or bridges, slab tracks are favored for their lower maintenance costs (Charoenwong et al., 2023). The structural differences between these track types result in varying behaviors, making the transitions between them a common source of maintenance (Sañudo et al., 2016). Figure 1 illustrates the different track types.

Figure 1: Ballasted and slab track respectively from left to right (TU Delft, n.d.)

The primary cause of issues within transition zones is the differential vertical movement, primarily resulting from plastic settlement of the ballast and sub-base. According to the literature, these settlements are caused by three factors: the loads imposed on the structure, the superstructure characteristics and the properties of the ballast, sub-ballast and sub-grade (Grossoni et al., 2021).

Variations in imposed loads, such as differing axle loads or vehicle speeds, and irregular behaviour of the ballast, sub-ballast, and sub-grade, often due to non-uniform densities, can result in disparities in settlement along the transition zone (Lundqvist & Dahlberg, 2005). These differences can lead to sleepers being connected to the rail without adequate support from the ballast, a condition commonly referred to as ”hanging sleepers”. Hanging sleepers can significantly compromise the integrity of the railway structure.

Hanging sleepers can cause noticeable impacts for trains traversing the section, leading to passenger discomfort and posing safety hazards such as derailment. Furthermore, hanging sleepers accelerate track deterioration by creating discontinuous track support, exciting the wheel-rail dynamic interaction. The undamped vibration of unsupported sleepers results in higher deflections and strains, ultimately shortening service lives (Zhu et al., 2011).

Typically, track damage prompts maintenance to realign the track. This is often done by the process of tamping, which involves lifting the track and raising the ballast surface to the required level. This is done by inserting vibrating tines that squeeze the ballast horizontally (Aingaran et al., 2018). While seeming initially effective, tamping disrupts the load-bearing structure and damages the individual ballast grains. This leads to even faster deterioration necessitating more frequent maintenance until complete track bed renewal is necessary. (Grossoni et al., 2021).

When corrective mitigation measures prove to be inadequate, preventive measures must be implemented to ensure that the soil bearing capacity is not exceeded. This entails optimizing the geometry of the transition zone to mitigate soil stresses as effectively as possible.

Previous research identified the optimal sleeper length to be around 3 meters, after which the stress did not reduce significantly. The width of the sleeper was also not found to be influential compared to the length. This was done with an ANSYS model containing a bridge and ballasted track (Masselink, 2023). However, this research designed the sleepers to have the same lengths and widths along the whole transition zone. In reality, this is not optimal, as the most critical part of the transition zone is close to the bridge in the model. This leads to over-designed sleepers further away from the bridge. The optimization was done for a single location of the train. This creates an unreliable optimized design if the location of the train changes. Finally, due to the deterministic nature of this design, uncertainties may cause it to fail.

2.2 Objective

The aim of this research is to determine the most influential design variables of a railway transition zone. This is done to minimize the number of variables that need to be optimized using time consuming optimization methods. In previous research, the sleepers of the transition zone were assumed to all have the same length and width. In this thesis, every sleeper will have its own length and width, creating a form of variability and uncertainty in the design. Therefore, the research question that is aimed to answer is:

How can the most influential design variables on the performance of a railway transition zone be determined using a static model while taking uncertainties into account?

To answer this question effectively, several sub-questions must be formulated that can provide valuable insights:

What are uncertainties and how can they be accounted for during design processes?

Understanding the uncertainties that could affect the railway structure is crucial for integrating them into the design of said railway structure. Understanding how uncertainty can be implemented into a design process is essential for designing reliable solutions to problems.

How can dynamic factors that influence the railway transition zone be implemented into a static model?

For this thesis, a static model will be provided. However, the real-life counterpart of this model will be conducted to many dynamic forces and vibrations. Finding ways to implement these dynamic forces may give more insight on the complex workings of the railway model.

How can the influence of the design variables of the railway transition zone be quantified using a static model?

To determine the most influential design variables, it needs to be determined how the influence of the design variables can be quantified.

3 Efficient Sampling Techniques for Stochastic Design Experiments

This chapter delves deeper into the methods for efficiently generating samples in stochastic design experiments. First, it compares deterministic and stochastic design methodologies, emphasizing the significance of effective sample creation in stochastic design. The chapter explores methodologies such as Design of Experiments (DOE) and Latin Hypercube Sapling (LHS), highlighting their roles in optimizing sample generation processes.

3.1 Design Methodologies

In the field of engineering, a multitude of design methodologies are employed to address the diverse challenges encountered during the design process. These methodologies provide distinct perspectives on the anticipated outcomes of a design, thus influencing the approach and techniques utilized. The selection of an appropriate design method depends on the significance of variability in the chosen variables. Among the most prevalent approaches in engineering are deterministic and stochastic design methodologies, both of which are integral to the creation of reliable and effective designs.

3.1.1 Deterministic Design Methodologies

In deterministic design, the outcome remains consistent given the inputs and conditions. However, in practical applications, uncertainties are always present, and deterministic design methods do not account for these uncertainties. To mitigate this limitation, safety factors are typically applied to each input parameter, resulting in a relatively conservative design. Despite this approach, the expected safety margin, reliability, and failure rate remain unknown (Halfpenny et al., 2019).

Optimizing for deterministic designs yields the optimal design for problems with fixed constraints and conditions. The deterministic constraints are represented by Equation 1:

$$G(\mathbf{x}) \leq 0 \tag{1}$$

Here, $G(\mathbf{x})$ is the performance function that describes the impact of the railway sleeper design on the performance of the transition zone. The vector **x** represents the design variables (Cavazzuti, 2013). In this research, these are the lengths and widths of the sleepers. Equation 1 specifies that a clear, unambiguous condition must be met. For instance, the designed sleepers should ensure that the soil settlement does not exceed 5 mm.

In deterministic design, the goal is to find the global solution to the problem. It is essential to prove that the identified optimum is indeed a global optimum and not merely a local one. Deterministic optimization is often preferred due to its computational efficiency and the accuracy of the solutions obtained (Cavazzuti, 2013). This approach is particularly suited for relatively simple problems, such as when the lengths and widths of all sleepers in the transition zone are uniform. In more complex scenarios with inherent uncertainties, stochastic design methods are more appropriate.

3.1.2 Stochastic Design Methodologies

Stochastic design incorporates uncertainty into the design process by using input variables with an expected value and probability distribution. Techniques such as Monte Carlo simulations are commonly employed, where different sets of variables are randomly selected to produce a smaller range of results. Post-processing these results yield designs that are not excessively conservative, unlike those produced using deterministic design approaches. An additional advantage of stochastic design methods is the clearer understanding of the impact of each implemented uncertainty (Halfpenny et al., 2019). Figure 2, illustrates a comparison between deterministic and stochastic design.

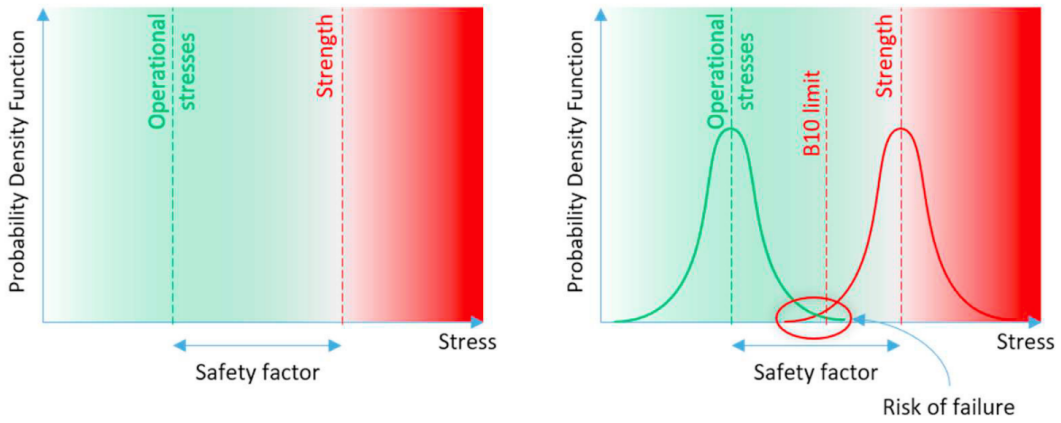

Figure 2: Comparison between deterministic and stochastic design (Halfpenny et al., 2019)

In contrast to deterministic optimization, Stochastic optimization can handle problems where randomness and uncertainty are present, closely mimicking real-world situations. Where deterministic optimization seeks a single optimal solution, stochastic optimization aims to find a solution that performs well on average across different combinations of uncertain variables. Consequently, solutions derived from stochastic optimization are less sensitive to changes. The strength of stochastic optimization lies in its ability to overcome local minima and explore the design space due to its inherent randomness. Additionally, stochastic methods can address multiple objectives simultaneously, a feat impossible for deterministic methods (Cavazzuti, 2013).

Developing a design that accounts for uncertainties tests the reliability of the design solution. Reliability is defined as the probability of a design fulfilling its purpose over a specified time period, effectively being the complement of the probability of design failure (Markine & Shevtsov, 2011). This approach transforms deterministic constraints into probabilistic constraints. Equation (2) demonstrates the transformation of Equation (1):

$$p_f = P[G(\mathbf{x}) \leq 0] = \int \dots \int_{D_f} f_x(\mathbf{x}) d\mathbf{x} \leq p^U \tag{2}$$

where **x** represents the vector of all design variables, and $G(\mathbf{x}) \leq 0$ signifies the failure condition. $f_x()$ is the joint density function of **x** and D_f is the integration region, also known as the failure domain, containing **n** failure criteria (Markine & Shevtsov, 2011). The upper boundary of the failure probability is denoted as p^U. This constraint implies that the probability of $G(\mathbf{x}) \leq 0$ must be less than than the failure probability. This method, known as reliability-based optimization, focuses on the probability of failure concerning constraints and the variation of the constraint functions (Koch et al., 2004).

Stochastic design is particularly well-suited for complex problems where real-life uncertainties and variabilities must be considered. It produces more robust designs that ensure safety and performance under real-world conditions. For instance, while a railway transition zone where each sleeper has the same length and width can be designed using deterministic approaches, more complex scenarios where each sleeper may have different dimensions necessitate stochastic design for optimization.

However, stochastic design does have some downsides, primarily concerning computation time. Although the optimized design can be highly effective, if it takes too long to compute, it remains an undesirable solution. This is especially critical since optimization is an iterative process, potentially causing significant delays in engineering projects. Therefore, selecting the right control parameters is crucial. This selection must be made carefully, as it significantly impacts the global behavior of the algorithm (Cavazzuti, 2013). Fortunately, several tools can assist in choosing the appropriate control variables, on of which is the Design of Experiments.

3.2 Design of Experiments

Design of Experiments (DOE) is a systematic methodology used to determine the relationship between factors affecting a process and the resulting output. The primary aim of DOE is to optimize design parameters within a defined design space, thereby maximizing the information obtained while minimizing resource usage. When applied correctly, DOE can significantly reduce computation time while maintaining accuracy in the process.

DOE is founded on three fundamental principles: randomization, replication, and blocking (Montgomery, 2013).

1. Randomization involves randomizing the assignment of experimental units to experiments and the order in which these experiments are applied. It helps mitigating the effects of uncontrolled variables by ensuring that these effects are evenly distributed across all experiments, which prevents systemic biases.

2. Replication means conducting independent, repeated runs of each factor combination. It improves the precision of the experiment by estimating the experimental error. This enhances the reliability of the result.

3. Blocking involves arranging experimental units into homogeneous groups, based on a factor that is not of primary interest to the experiment but could potentially cause nuisances. By keeping these nuisance factors into account, the variability of the result is minimized, which increases the experiment's accuracy.

In this research, variations of Monte Carlo sampling techniques will be employed to generate random samples of lengths and widths of railway sleepers, encompassing the design space. This design space constitutes the DOE framework. The impact of these samples on soil settlement and stresses will then be analyzed using an ANSYS model, which will be further detailed in Chapter 4. The most critical sleepers will subsequently be reintegrated into to the DOE for further optimization.

3.3 Monte Carlo Sampling in Complex Design Spaces

In relatively simple design spaces, numerical methods such as direct numeric integration can effectively estimate the probability of failure for specific designs. However, as design spaces become more complex with additional variables, these methods become impractical or infeasible. Monte Carlo simulations (MCS) are commonly employed in such scenarios. The failure probability, as described in Equation 2, is calculated by assigning random values to the variables in **x**. This process is repeated N times, where n denotes the number of failures, to estimate the probability of failure, given by the ratio n/N. This process is described by Equation 3 (Markine & Shevtsov, 2011):

$$p_f \approx \frac{1}{N} \sum_{j=1}^{N} G(\hat{\mathbf{x}}_j) \leq 0 \tag{3}$$

This equation sums up the number of failures and divides it by the total number of experiments. Achieving reliable MCS requires a substantial number of samples due to their random selection, which may not comprehensively cover the entire design space, as illustrated in Figure 3.

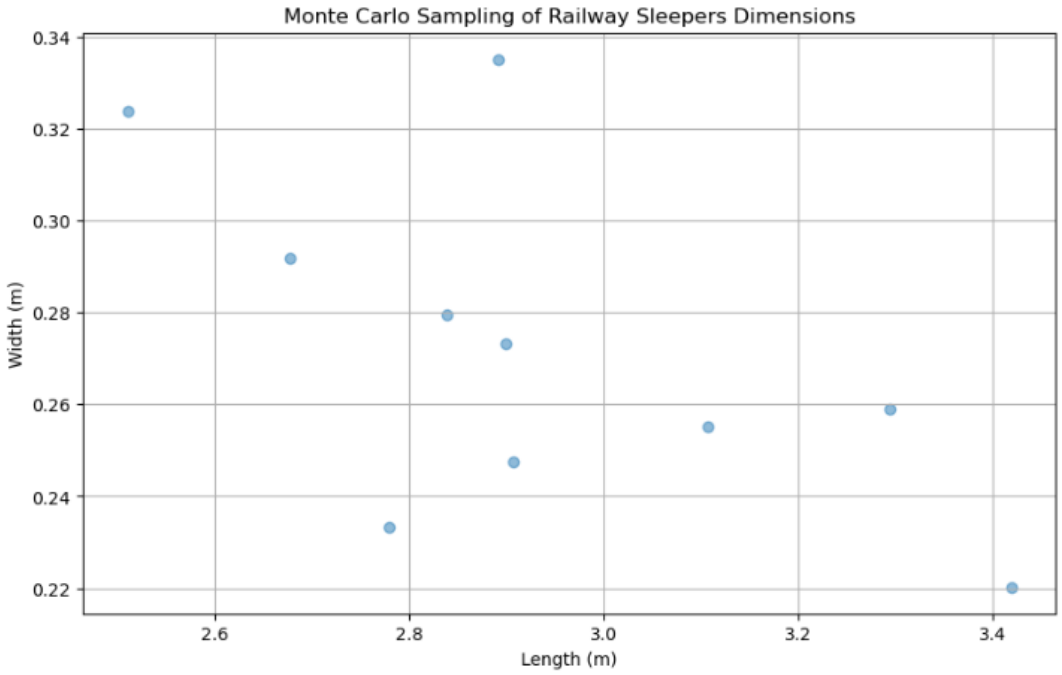

Figure 3: Monte Carlo sampling with ten samples

Figure 3 demonstrates that ten randomly chosen samples do not fully cover the design space, potentially providing an incomplete understanding of how design variables influence output variables. While the quality of MCS can be adequate with a smaller number of samples, this is not guaranteed due to its stochastic nature. To mitigate variance in MCS, a large number of samples must be taken to ensure thorough coverage of the design space (Markine & Shevtsov, 2011). While efficient for designs involving fewer variables, this approach becomes increasingly inefficient with more variables, necessitating alternative methods to reduce variance. One such method employed in this research is Latin Hypercube Sampling.

3.4 Optimized Latin Hypercube Sampling

Latin Hypercube Sampling (LHS) is a variant of MCS that employs variance reduction techniques to effectively cover the entire design space with fewer samples. This method divides the design space into n sections of equal probability. For N variables, the total number of sample points in the design space is n^N. However, due to computational constraints, only n samples are selected and distributed across the sample space in a manner that ensures each section contains exactly one sample point. This approach is computationally efficient for generating samples in design problems but lacks robustness, as it does not guarantee complete coverage of the design space (Thomson & Martins, 2011). The concept of LHS is illustrated in Figure 4.

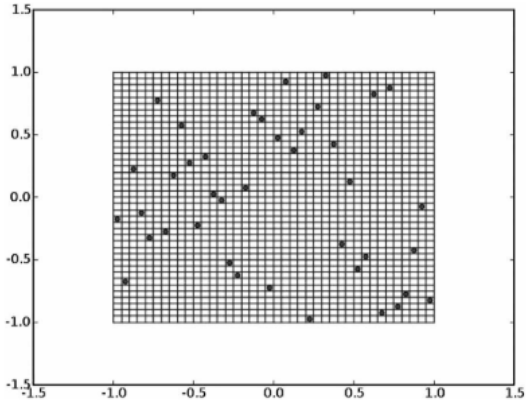

Figure 4: Latin Hypercube Sampling with 40 points (Thomson & Martins, 2011)

Figure 4 demonstrates that while LHS attempts to distribute points evenly, the placement may still appear random. leading to potential lower quality of sampling points and diagonal correlations between points. To enhance LHS, Optimal Latin Hypercube Sampling (OLHS) maximizes the minimum distance between sampling point, as shown in Figure 5.

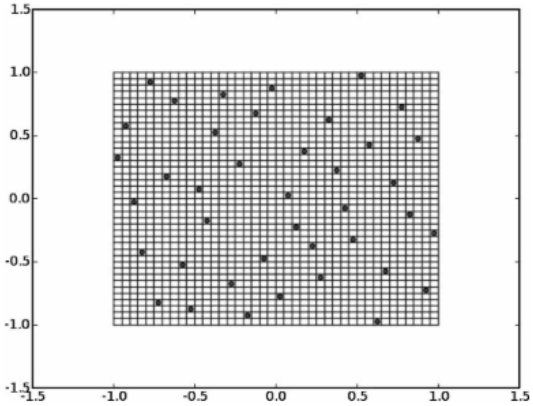

Figure 5: Optimized Latin Hypercube Sampling with 40 points (Thomson & Martins, 2011)

Figure 5 illustrates how OLHS improves upon LHS by achieving a more uniform distribution of sample points across the design space, ensuring better representation of every design variable. However, a drawback compared to regular LHS is increased computation time due to the need for optimizing sample distribution. Balancing between sample quality and quantity is crucial, as additional samples, variables, and optimization iterations inevitably increase computation time. Finding this balance is essential for efficient application in engineering optimization tasks.

3.5 LHS implementation in Python

For the upcoming Ansys experiment, various samples of railway sleeper dimensions, spanning different lengths and widths, need to be generated. This task is accomplished using the lhs-function from pyDOE2 package in Python. This function requires several input parameters to operate effectively.

- n (number of input parameters)
- samples (number of samples generated)
- criterion (optimization criterion)
- iterations (the number of iterations)

Initially, LHS is conducted using only two design parameters. Omitting the specification of ”criterion” and ”iteration” defaults to regular Latin Hypercube Sampling. As depicted in Figure 6, sample points are randomly distributed across the design space, with the minimum distance histogram indicating uneven coverage.

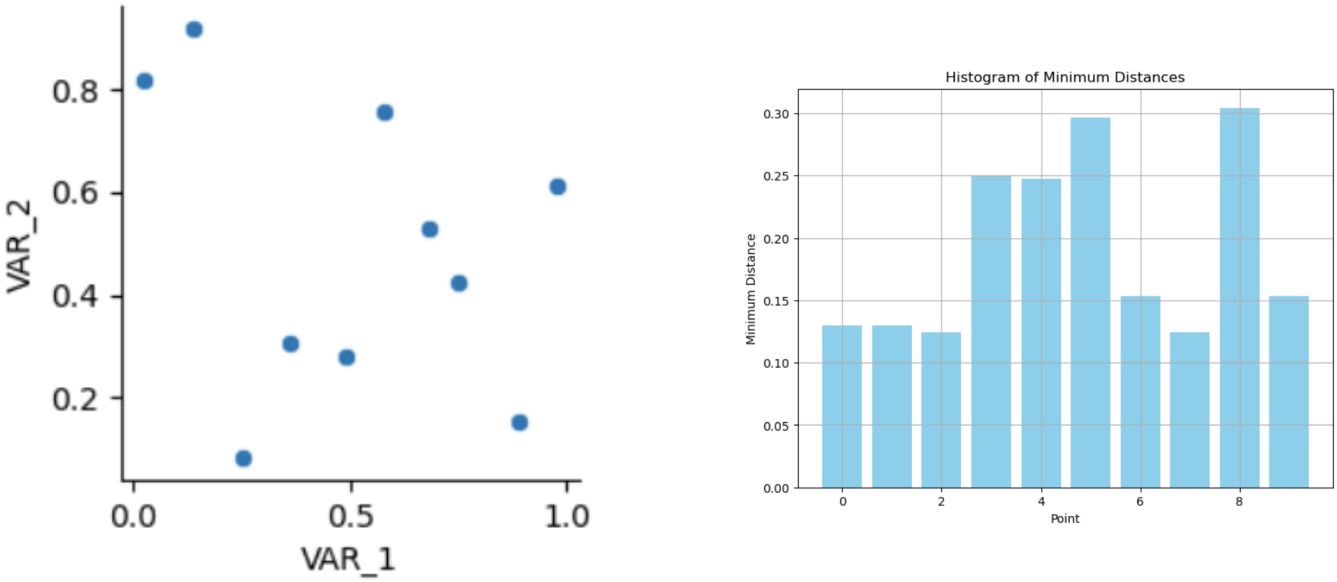

Figure 6: Points distributed over design space (left) and minimum distance between points (right)

To ensure adequate representation of both variables, optimization options within the lhs-function are utilized. These options include defining an optimization criterion and determining the number of iterations. Achieving a balance between sample quality and computation time is crucial. For instance, in a two-variable scenario, 100,000 iterations were found suitable. The ”centermaximin” criterion was employed to maximize the distance between sample points while ensuring they remain centered within their intervals, thereby achieving a balanced coverage of the design space. Figure 7 illustrates the optimized design space and maximum distance plots resulting from these adjustments.

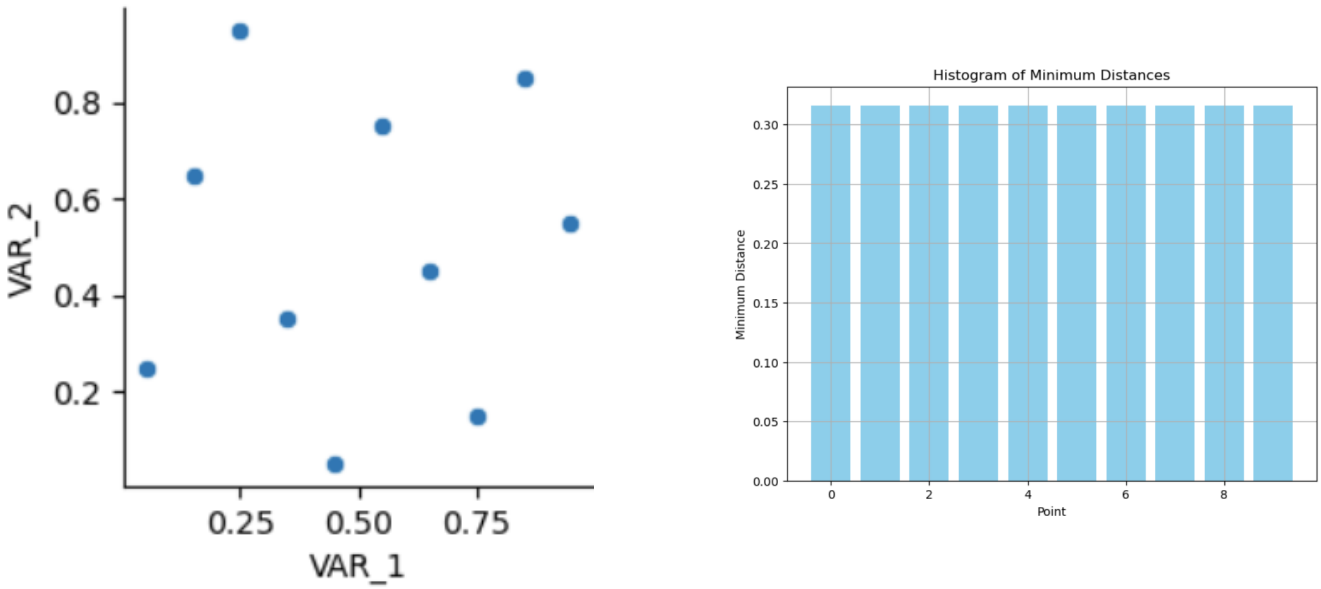

Figure 7: Points distributed over design space (left) and minimum distance between points (right)

In the context of a railway transition zone, multiple design variables are employed. Specifically, two variables per sleeper. Despite the increase in dimensions of the design space, the fundamental principle of LHS remains unchanged. To demonstrate its applicability in higher dimensions, LHS was tested in a 5-dimensional design space. However, as the number of variables increases, computation times escalate significantly. While generating samples for two variables with 100,000 iterations takes seconds, the same process for five variables requires minutes. This necessitates adjusting the iteration count for higher dimensions, which may slightly compromise sample quality.

Visualizing the coverage and quality of the design space becomes challenging beyond three dimensions due to limitations in human spatial comprehension. To assess sample quality, minimum distance plots, such as the one depicted in Figure 8 are utilized in this research. Uniformity in minimum distances across the design space suggests higher sample quality.

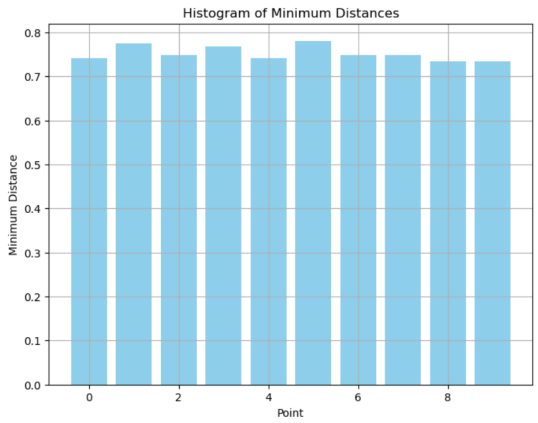

Figure 8: Minimum distance plot for OLHS with 5 variables

4 Static Modeling of Railway Track Dynamics and Transition Zones

This chapter explores the application of static modeling techniques to analyze the behavior of railway tracks under varying train positions. It discusses the constraints and parameters used in the model, including sleeper dimensions and train locations within transition zones. The chapter examines how static models simulate dynamic effects and account for factors such as track stiffness changes near steel structures. Limitation of static modeling compared to dynamic simulations are also discussed.

4.1 Model Description and Parameters

In this research, a model of a railway transition zone provided by Dr. V.L. Markine will be employed. Before proceeding with experimental investigations, it is imperative to gain a comprehensive understanding of this model. The model is written in the Ansys Parametric Design Language (APDL), a specialized programming language designed for interfacing with the Ansys Mechanical software. The utilization of APDL affords the opportunity to implement various modifications to the original model. Furthermore, it enables a Python script to automatically adjust design variables, execute the Ansys model, and store the resulting data. This automation significantly enhances the efficiency of the model evaluation.

In Figure 10, the original model that was provided by Dr. V.L. Markine is illustrated. The model can be segmented into two distinct components. The first component comprises the ballasted track, which includes a ballast bed and a soil layer. The second component represents a slab track situated on a bridge, with the bridge is modelled as a steel slab. The area of the ballasted track adjacent to the steel construction is designated as the transition zone. Both segments of the model incorporate defined sleepers and rails. Each component of the model is assigned specific material properties, including a Young's modulus, Poisson's ratio, and density. These properties must be specified prior to executing the model.

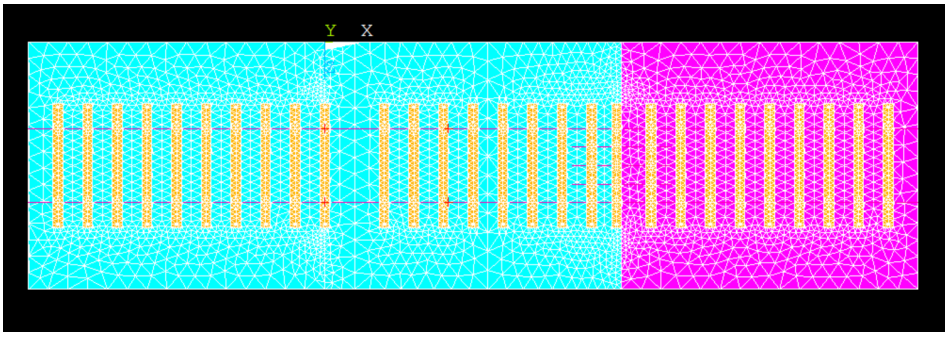

Figure 9: Ansys model, ballasted track, transition zone, slabbed track from left to right.

To execute the mode, several supplementary parameters are required. These parameters include the load exerted by the train on the railway track, the distance between the front and rear wheels of the bogie, and the position of the foremost wheel of the train in relation to the ballasted track zone. Upon providing these inputs, the model can be resolved, producing two specific outputs: the maximum stress and the vertical deformation of the soil and ballast.

The experiment utilizing this model aims to identify the railway sleepers that are most critical for optimization. The objective is to minimize the number of sleepers requiring optimization during the optimization process by omitting the sleepers deemed less impactful. The methodology for this experiment will be described in section 5.3. The fundamental premise of the experiment is that larger sleepers will result in reduced stresses in the ballast and subsoil. This outcome is attributed to the

increased contact area, which facilitates a more uniform distribution of loads, thereby leading to lower stress. The relationship is expressed in equation 4.

$$\sigma = \frac{F}{A} \tag{4}$$

To validate the functionality of the model, this relationship was empirically tested. The length of the sleepers varied between 1.6 m and 4.0 m, and the width varied between 0.1 m and 0.4 m, while maintaining all other variables constant. The resulting stresses in the subsoil for the different lengths and widths of the sleepers are presented in Table 1 and Table 2, respectively.

Table 1: Stress and Von Mises stress at different lengths (width at 0.25 m)

Length [m]	Stress [10^5 N/m²]
1.838	6.5
1.856	6.7
2.132	5.8
2.526	5.1
2.730	4.8
2.851	4.9
3.189	5.0
3.297	5.0
3.742	4.8
3.949	4.7

Table 2: Stress and Von Mises stress at different widths (length at 2.5 m)

Width [m]	Stress [10^5 N/m²]
0.110	5.0
0.144	5.4
0.183	5.2
0.219	5.0
0.243	5.0
0.278	5.0
0.303	5.1
0.330	5.2
0.360	5.1
0.385	5.1

It can be observed that the stresses significantly decrease for lengths between 1.8 m and 2.5 m. However, increasing the length beyond this range yields diminishing returns, which is in line with the previous research of Masselink (Masselink, 2023). This may be attributed to the bending moment exerted by the train on the sleeper, which causes excessive deformation. The bending stiffness of the sleepers may be insufficient, leading to greater forces concentrated in the middle of the sleeper (Balabušić et al., 2019). The width appears to have very little impact on the stresses in the soil at these lengths. When testing this on sleepers with a length of 1.6 m, the widths seem to have a more pronounced effect. However, the stresses remain higher compared to using a length of 2.5 meters. Therefore, the length of the sleeper seems to be more crucial, as it increases the area of the sleeper more significantly.

4.2 Static Modeling of Dynamic Railway Track Interactions

In real-life scenarios, a railway track experiences dynamic forces which vary significantly based on time dependent factors such as train speed and acceleration, and the location of the train on the track. However, in this study, a static model is employed to analyse the stresses and settlements in the ballast and soil under specific train positions.

To simulate the dynamic effects using a static model, the position of the train is iteratively adjusted for each analysis. By varying the train's location, the model calculates the corresponding stresses and settlements, mimicking the varying load conditions that would occur over time in a dynamic setting.

To replicate dynamic interactions near steel structures, an additional measure is implemented into the model. Throughout the operational lifespan of railway the railway transition zone, trains frequently transition between slab tracks and ballast track. As previously discussed, the abrupt change in track stiffness induces heightened loads near bridges within the transition zone due to dynamic effects. The loading experienced by the ballast and soil during these transitions leads to progressive softening of these materials over time. Consequently, settlement in these regions tend to be more pronounced. In order to emulate this softening, adjustments are made to the model to reduce the soil stiffness adjacent to the steel construction. The length of this section is 3 m. In figure 10, the model with the softened soil is illustrated.

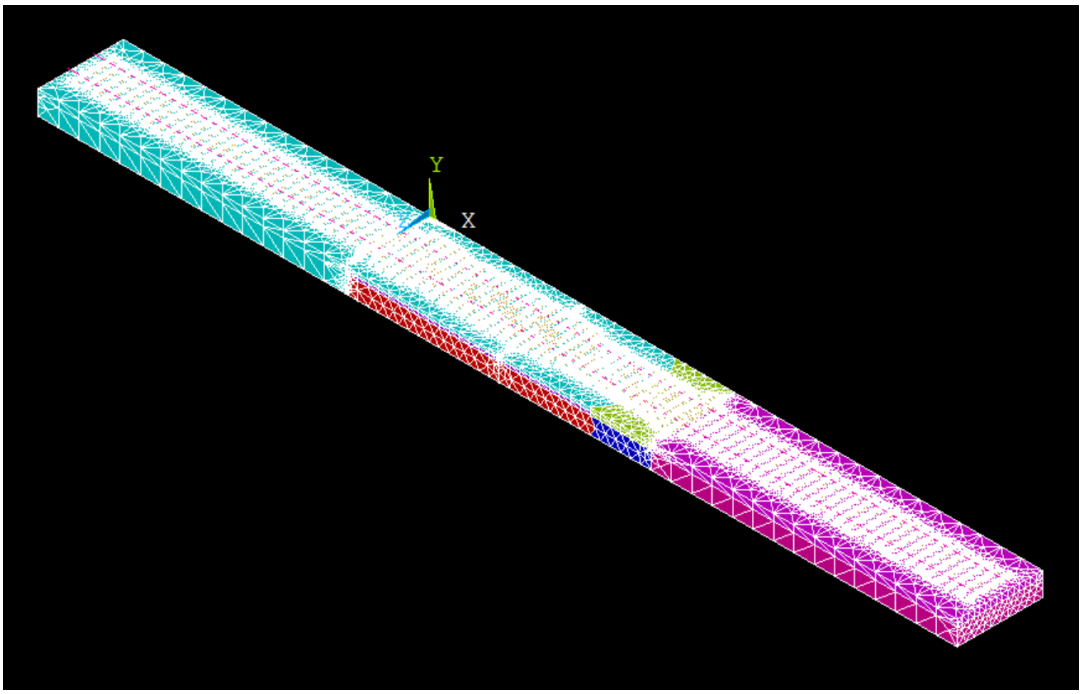

Figure 10: Ansys model, with softer ballast and soil (light green and dark blue respectively)

It has to be noted however, that a static model is limited compared to a dynamic simulation. A static model simplifies the dynamic processes that are normally present into discrete analyses under specific train positions. This causes long-term effects, such as long-term settlement patterns and stress distributions to be predicted inaccurately. The model also does not account for dynamic amplifications that might occur in the soil structure due to train movements. This can underestimate peak stresses and deformations.

4.3 Constraints on Model Variables

The constraints imposed on the model variables are derived from real-life examples and modeling limitations. For instance, the sleeper length must exceed the average track gauge of 1435 mm in the Netherlands, plus additional space for rail fasteners, resulting in a minimum length of approximately 1600 mm. The maximum length of the sleepers is restricted by the model to 4000 mm. However, as shown in Table 1, lengths shorter than 2500 mm result in significantly higher stresses in the soil, indicating they are suboptimal due to the excessive stresses generated. Conversely, sleepers of much greater length do not significantly impact stress reduction. Consequently, only sleepers with lengths between 2500 mm and 3500 mm will be considered. This constraint is formulated in equation 5.

$$2.500m \leq L \leq 3.500m \tag{5}$$

The width of the sleepers is also constrained by minimum and maximum values. In Ansys, the minimum value is set to 100 mm. However, to allow sufficient space for fasteners, a minimum value of 300 mm is used. The maximum width is limited to prevent the sleepers from touching each other, which would effectively create a slab track. Thus, the sleepers should be spaced appropriately. In the Netherlands, the regular spacing of railway sleepers is 600 mm. Considering a minimum distance of 2500 mm between the sleepers, the maximum allowable width is 400 mm. This constraint is expressed in equation 6.

$$0.300m \leq W \leq 0.400m \tag{6}$$

The is on additional constraint concerning the location of the train, which changes with each evaluation of the model, as described in Section 4.2. To simulate the train traversing the entire transition zone, the initial position should be just before the transition zone, and the final position should be just after exiting the zone. The total length of the transition zone is 18 meters. The location is defined as the position of the rear wheel of the bogie relative to the border of the transition zone and the regular ballasted track. Therefore, the positional parameter should be set at -2.5 meters to position the train just before entering the transition zone. This constraint is formulated in equation 7.

$$-2.500m \leq PT \leq 18.000m \tag{7}$$

5 Experimental Setup and Methodology

This chapter outlines the final preparatory steps leading up to the experiment, as well as the experimental workflow. Initially, stress and settlement analysis are conducted at various locations along the train's path. Following this, samples for the experiment are generated using Optimized Latin Hypercube Sampling (OLHS). Lastly, the experimental setup is detailed.

5.1 Examination of the Stress and Settlement

To determine the most critical railway sleepers within the transition zone, a multi-step methodology was employed. Initially, the concept of the driving train, explained in Section 4.2, was tested. The sleeper dimensions were kept uniform throughout the model's length, ensuring that variations in the model were solely due to changes in the location of the applied forces during each evaluation. This approach facilitates the identification of anomalies within the model.

To evaluate the model's performance, the location of the applied forces was systematically varied in 20 increments from -2.5 meters to 18 meters, as described in Section 4.3. Subsequently, the resulting maximum stress and deformation corresponding to each force location were plotted to verify their conformity with expected behaviour. In Figure 11, these plots are illustrated.

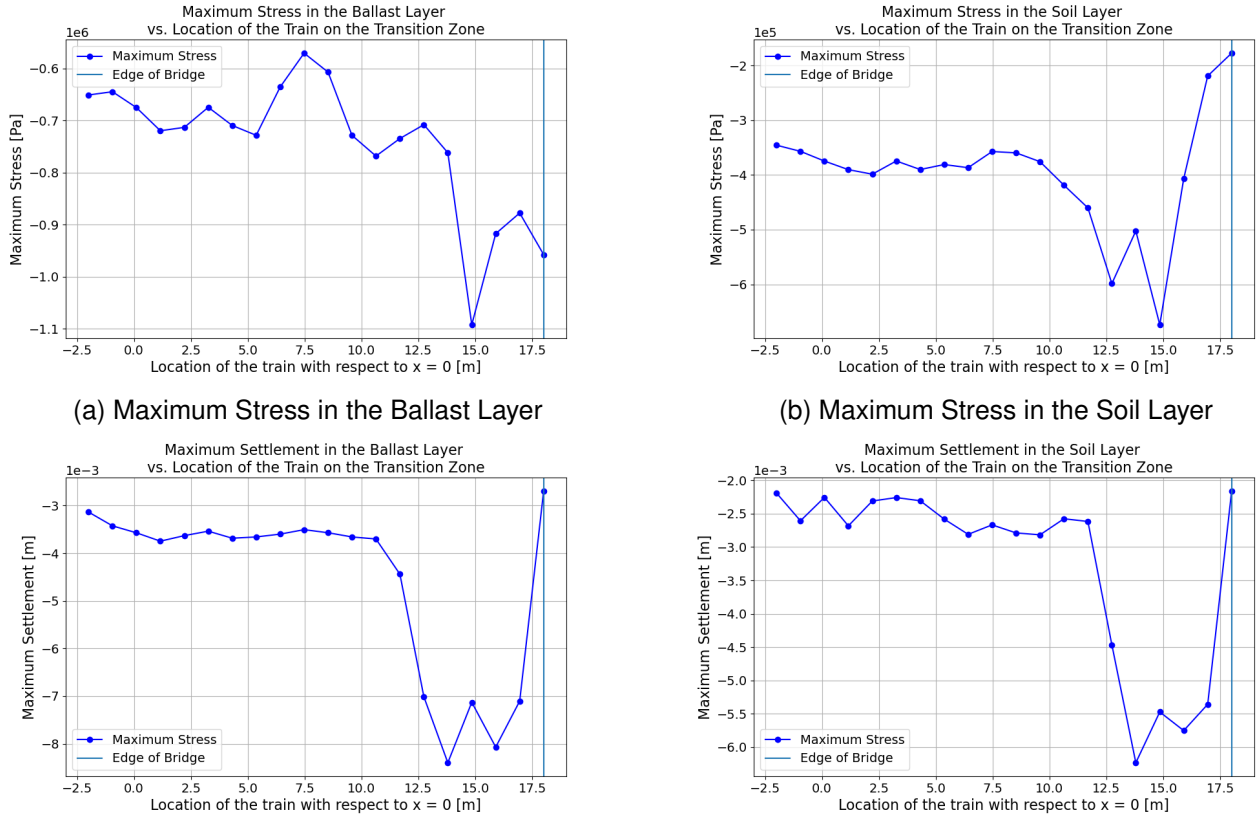

(a) Maximum Stress in the Ballast Layer

(b) Maximum Stress in the Soil Layer

(c) Maximum Settlement in the Ballast Layer

(d) Maximum Settlement in the Soil Layer

Figure 11: Maximum stress and settlement values against the location of the train.

A more thorough examination is conducted at the location of the maximum stresses and settlement. First, the stresses are examined. Figure 12 illustrates the stresses within the ballast layer of the Ansys model, resulting from the rear wheel of the train positioned at x = 14.842 meters. This figure reveals that the maximum stress occurs adjacent to the bridge. This phenomenon can be attributed to the lower stiffness of the soil next to the bridge. Soil with lower stiffness exhibits reduced resistance to settlement, whereas a bridge, with its relatively high resistance, undergoes minimal deformation. This discrepancy in deformation between the bridge and the adjacent soil likely causes the increased stresses observed in the soil.

The highest stress at this specific location is attributed to the proximity of the front wheel of the train to the bridge. When the front wheel is closest to the bridge, it induces the greatest settlement in the soil immediately adjacent to the bridge. This increased settlement results in higher stresses in the soil compared to other locations. In the soil layer, the highest stress is found between the normal soil and the softer soil, which may also be caused by the settlement disparity.

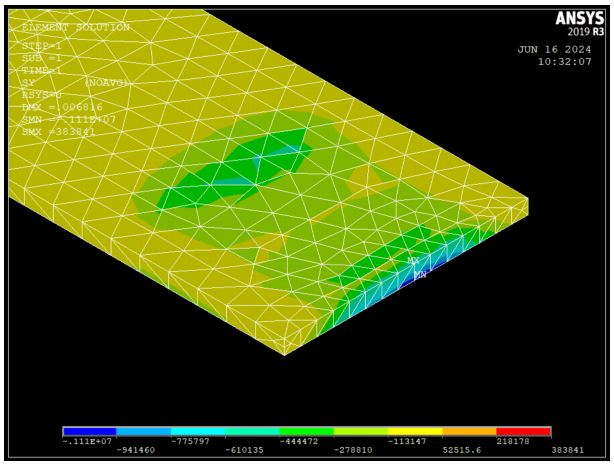

Figure 12: Stresses in the ballast layer at train location x = 14.842 m

When examining settlement patterns, it is logical that the highest deformations occur in the softer soil due to their lower load-bearing capacity and higher compressibility, which increase settlement. The maximum settlement is observed at location x = 13.789 meters, which lies outside of the area of soft soil for the rear wheel. However, the front wheel is positioned in the middle of the soft soil area, as depicted in Figure 13. This concentration of load in the soft soil section leads to the maximum settlement in this region.

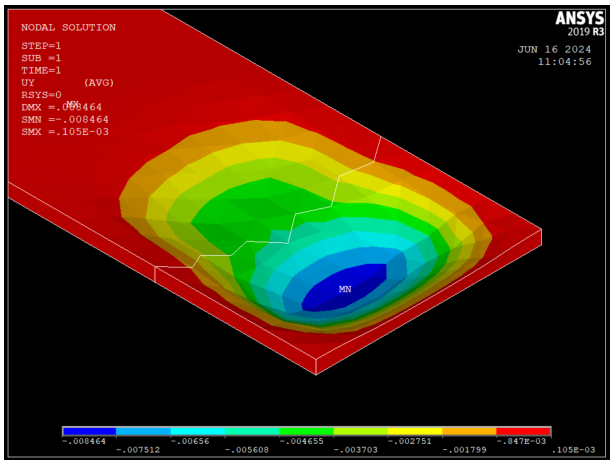

Figure 13: Settlement in the ballast layer at train location x = 13.789 m

5.2 Creating OLHS Samples

Samples for the model are generated using OLHS, following the procedure outlined in Section 3.5. The model consists of 31 sleepers, each characterized by two variables: length and width. This gives rise to 62 variables, resulting in a 62-dimensional parameter space. In total, 10 samples were generated for the experiment.

Currently, the sample values range from 0 to 1 due to the nature of LHS, which generates samples within the unit cube $[0, 1]^d$, where d is the number of dimensions. Consequently, each variable needs to be scaled appropriately. This scaling can be performed using Equation 8:

$$x_{scaled} = a_i + x_{lhs} \cdot (b_i - a_i) \tag{8}$$

where x_{scaled} is the scaled variable, x_{lhs} is the original LHS sample value between 0 and 1, a_i and b_i are the lower and upper bound of the target range specified in Equation 5 and Equation 6. Scaling each sample according to its respective target range ensures that the 10 samples will have 31 lengths and widths within the specified ranges. These samples are detailed in Appendix A.
To assess the quality of the samples, a minimum distance plot is generated. This plot is illustrated in Figure 14. This plot illustrates that the distances between the samples are relatively even, indicating that they are evenly spaced in the design space.

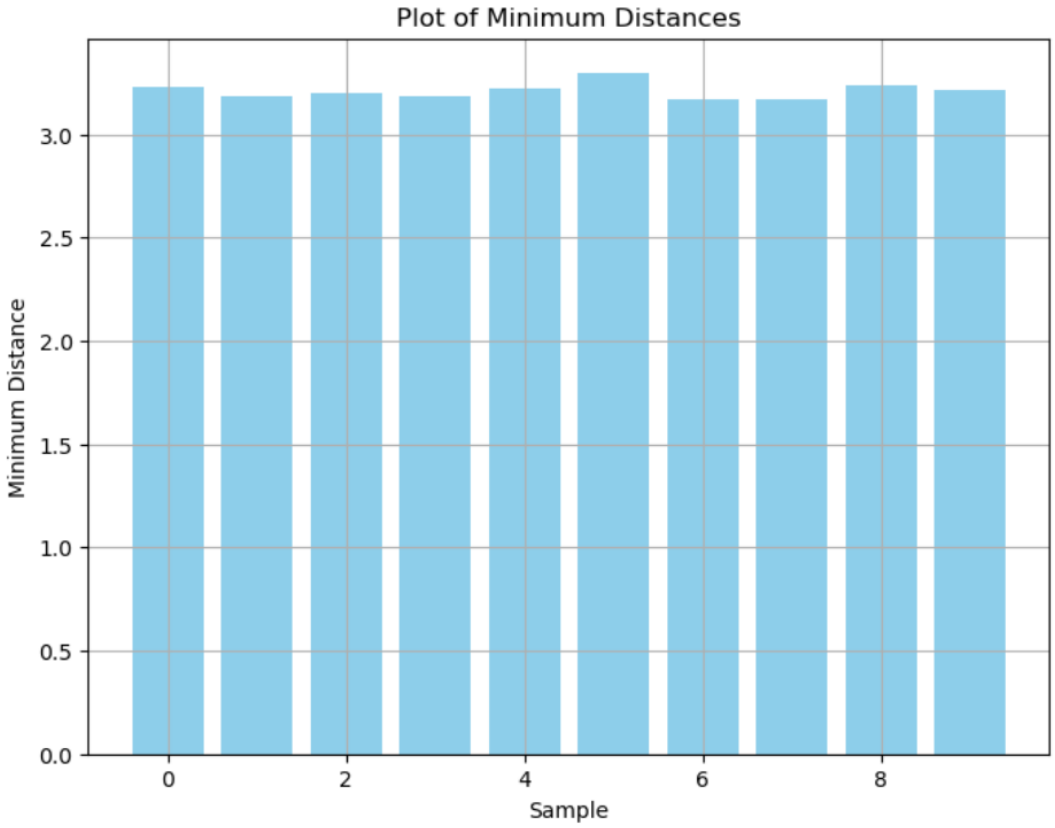

Figure 14: Minimum distance plot of the scaled OLHS samples.

5.3 Description of the Experiment

To identify the most critical sleepers within the transition zone, the variables for length and width from an OLHS sample are used as input variables for the Ansys model. The model is then executed multiple times, each run varying the train's position as previously described. By identifying the location with the maximum stress or settlement in each run, the most critical location for each sample can be determined. This procedure is repeated for every generated sample, resulting in a critical location with corresponding stress and settlement for each sample.

Subsequently, the sample associated with the highest stress and/or settlement is identified, revealing a configuration of sleeper lengths and widths that leads to this behavior. According to Equation 4, sleepers with a smaller area are expected to result in higher stress and, consequently, greater settlement. Thus, the configuration exhibiting the lowest lengths and widths around the critical area should be emphasized.

6 Results

This chapter presents the findings of the experimental investigation. The maximum stress and settlement values obtained for each sample are put into dedicated tables to facilitate identification of the samples exhibiting the most favorable and least favorable performance. A more thorough examination of these results will be given in the discussion.

6.1 Stress

The maximum stress experienced within both the ballast and soil layers was determined, as elaborated upon Section 5.1. Each sample was evaluated across the transition zone, resulting in a location exhibiting the highest stress. Table 3 details the maximum stress observed within the ballast layer and its corresponding location. As mentioned earlier, the sample values are located in Appendix A.

Table 3: Location of the maximum stress in the ballast.

Sample	Location (m)	Max Stress Ballast (N/m²)
1	14.842105	-1099429.07
2	14.842105	-1076820.98
3	14.842105	-1099383.86
4	14.842105	-1082429.47
5	14.842105	-1111140.82
6	14.842105	-1116820.71
7	14.842105	-1104560.18
8	14.842105	-1080991.05
9	14.842105	-1068562.56
10	14.842105	-1118265.22

The data within Table 3 reveals a consistent location for peak stress across all samples, aligning with the findings presented in Section 5.1. Sample 10 exhibits the highest maximum stress value, while Sample 9 demonstrates the lowest.

Following the same approach, the influence of different samples on the maximum stress within the soil layer was investigated. The corresponding results are presented in Table 3. Here, Sample 5 clearly represents the scenario with the highest stress level. Conversely, Samples 1, 8 and 9 demonstrate lower stress values.

Table 4: Location of the maximum stress in the soil.

Sample	Location (m)	Max Stress Soil (N/m²)
1	14.842105	-598817.06
2	14.842105	-613444.48
3	14.842105	-608644.22
4	14.842105	-628017.40
5	14.842105	-652290.49
6	14.842105	-616339.13
7	14.842105	-604552.62
8	14.842105	-598640.13
9	14.842105	-599627.26
10	14.842105	-629545.84

6.2 Settlement

The methodology employed for analyzing maximum stress was replicated to assess the impact of the samples on maximum settlement. The results corresponding to the ballast are presented in Table 5.

Table 5: Location of the maximum settlement in the ballast.

Sample	Location (m)	Max Settlement (m)
1	13.789474	0.007840
2	13.789474	0.008052
3	13.789474	0.007928
4	13.789474	0.008043
5	13.789474	0.008077
6	13.789474	0.008004
7	13.789474	0.007982
8	13.789474	0.007915
9	13.789474	0.007927
10	13.789474	0.008080

The location of maximum settlement exhibited a slight deviation from the location of the maximum stress, as explained in Section 5.1. Sample 10 demonstrates the largest maximum settlement. However, the overall variation between samples is minimal, with a difference of approximately 0.2 mm observed between the samples with the highest and lowest settlement values.

Similar to the stress analysis, the maximum settlement within the soil layer was evaluated. The corresponding results are presented in Table 6. These findings indicate that Sample 4 experiences the highest settlement, followed closely by Samples 5 and 10. Conversely, Samples 1 and 9 exhibit the lowest settlement values.

Table 6: Location of the maximum settlement in the soil.

Sample	Location (m)	Max Settlement (m)
1	13.789474	0.005745
2	13.789474	0.005852
3	13.789474	0.005812
4	13.789474	0.005972
5	13.789474	0.005950
6	13.789474	0.005845
7	13.789474	0.005788
8	13.789474	0.005815
9	13.789474	0.005745
10	13.789474	0.005922

7 Discussion

The results of the experiment yielded various samples that return the highest stress and settlement concentrations. While the hypothesis initially anticipated a correlation between larger sleeper areas and lower stresses, the results do not support this relationship. Examining the locations of peak forces, a potential association was anticipated between lower sleeper dimensions and higher stress or settlement values. This was not consistently observed.

An explanation may come from Section 4.1. This section shows that length does not significantly decrease the stress and settlement in the soil after reaching a length of 2.5 meters. The reason that was given for this was that the bending moment imposed on the sleeper by the train load would be too high for the sleeper to handle without excessive bending. Leading concentrated load in the middle of the sleeper. If this is indeed the case, longer sleepers with the same bending stiffness will have no effect except for using more materials. This hypothesis may be tested by increasing the stiffness of the sleepers, or increasing the height of the sleeper. With a higher bending stiffness, the bending moment resistance should be higher, leading to less deformation in the middle of the sleeper. If the hypothesis is indeed true, the stress in the ballast and soil should decrease.

Assuming minimal influence of sleeper length and width on the results suggests the potential significance of other factors beyond sleeper geometry. This is further supported by the observed variation in maximum stress and settlement values across different samples. A potential hypothesis proposes a correlation between significant disparities in adjacent sleeper lengths and higher stress concentrations. Notably, the location exhibiting peak stress coincides with a notably higher disparity in adjacent sleeper lengths for samples with elevated stress with elevated stress compared to those with lower stress. This disparity could be attributed to variations in bearing surface area, with longer sleepers distributing the load from the rails over a larger zone compared to shorter sleepers. A significant difference in bearing surface areas could lead to uneven settlement and consequently, higher stress levels. However, definitive validation of this hypothesis needs further experimentation. Future research could focus on isolating the most critical section of the transition zone and systematically varying the length differences between adjacent sleepers.

Regarding the model that was used, some uncertainties are present in how well the results of the experiment represent the real stresses and settlement that occur in the railway transition zone. Because the model remains a static model, even though some efforts of implementing dynamic factors were done, complex dynamic factors are not taken into account. These factors are for example the inertia and speed of the train, and the possible resonance that can occur if the train matches the natural frequency of the train. These effects are difficult to accurately represent in a static model. However, they can greatly amplify the loads acting on the transition zone. To create a better understanding of these factors, a more complex model may be used in the future.

Finally, the computation time of the experiment conducted in the thesis took quite a long time. In total, 200 evaluations were made to get a good idea of the location of the maximum stress and settlement in the transition zone for each sample. With each evaluation taking around 10 seconds, the total evaluation time took between 40 minutes and 1 hour. For one evaluation, this is fine. However, in iterative processes, this may take too long. This research has shown that the maximum stresses and settlement of the soil should occur close to the bridge in the transition zone. Zooming in to this area for future research by shortening the transition zone, will create model where less railway sleepers and less sample points are needed. This will reduce computation time significantly.

8 Conclusion

The objective of this thesis was to answer the research question "*How can the most influential design variables on the performance of a railway transition zone be determined using a static model while taking uncertainties into account?*" To answer this question, an analysis on how to implement uncertainties into design was done; a static Ansys model was adapted to try and implement dynamic factors into it; a Python script was made to give input values to this model, run the model and review the model.

The analysis on uncertainties showed that stochastic design can be used to create solutions that are resilient to variability. However, it also showed that computation time is often an issue when utilizing stochastic optimization. To reduce this, sampling techniques such as Design of Experiments and Monte Carlo Sampling are often used. Monte Carlo Sampling has problems when a high number of variables are present in the design space. Therefore, variance reduction techniques such as Latin Hypercube Sampling are used.

By creating Latin Hypercube Samples using a Python script, samples of 31 railway sleepers with different widths and lengths could be put into an Ansys model. This model then proceeded to calculate the highest stress and settlement in the ballast and soil layer underneath the railway track for 20 different locations on the transition zone. This is done for 10 samples, which lead to maximum stress and settlement in both the ballast and soil layer. Both the maximum stress and settlement was measured within 5 meters adjacent to the bridge. This proves that this area is the most critical part of the railway transition zone.

The hypothesis was that sleepers with a higher area result in a lower stress in the soil and ballast layers. However, when comparing the samples with the highest and lowest stress and settlements, this hypothesis was not true all of the time, as the sleepers around the loading area of the high-stress samples often had higher areas than the low-stress samples. Looking at the results, the highest settlements and stresses often occurred when adjacent sleepers had a large disparity in length. This may be because of differences in the bearing surface area, which results in uneven settlement and thus stress. If this is correct, gradual increases and decreases of railway sleeper length should be an important design variable to keep in mind during optimization. However, to confirm this hypothesis, more research has to be done.

For other future research, other ways of implementing dynamic factors in the static model can be thought of. For example, increasing the load close the bridge to simulate the small drop or rise that usually occurs when transferring from slab track to ballasted track.

References

Aingaran, S., Le Pen, L., Zervos, A., & Powrie, W. (2018). Modelling the effects of trafficking and tamping on scaled railway ballast in triaxial tests. *Transportation Geotechnics*, *15*, 84–90. https://doi.org/10.1016/j.trgeo.2018.04.004

Balabušić, M., Folić, B., & Ćorić, S. (2019). Bending the Foundation Beam on Elastic Base by Two Reaction Coefficient of Winkler's Subgrade. *Open Journal of Civil Engineering*, *09*(02), 123–134. https://doi.org/10.4236/ojce.2019.92009

Cavazzuti, M. (2013). *Optimization Methods: From Theory to Design Scientific and Technological Aspects in Mechanics*. Springer Berlin Heidelberg. https://doi.org/10.1007/978-3-642-31187-1

Charoenwong, C., Connolly, D., Colaço, A., Alves Costa, P., Woodward, P., Romero, A., & Galvín, P. (2023). Railway slab vs ballasted track: A comparison of track geometry degradation. *Construction and Building Materials*, *378*, 131121. https://doi.org/10.1016/j.conbuildmat.2023.131121

Grossoni, I., Powrie, W., Zervos, A., Bezin, Y., & Le Pen, L. (2021). Modelling railway ballasted track settlement in vehicle-track interaction analysis. *Transportation Geotechnics*, *26*, 100433. https://doi.org/10.1016/j.trgeo.2020.100433

Halfpenny, A., Chabod, A., Czapski, P., Aldred, J., Munson, K., & Bonato, M. (2019). Probabilistic Fatigue and Reliability Simulation. *Procedia Structural Integrity*, *19*, 150–167. https://doi.org/10.1016/j.prostr.2019.12.018

Koch, P., Yang, R.-J., & Gu, L. (2004). Design for six sigma through robust optimization. *Structural and Multidisciplinary Optimization*, *26*(3), 235–248. https://doi.org/10.1007/s00158-003-0337-0

Lundqvist, A., & Dahlberg, T. (2005). Load impact on railway track due to unsupported sleepers. *Proceedings of the Institution of Mechanical Engineers, Part F: Journal of Rail and Rapid Transit*, *219*(2), 67–77. https://doi.org/10.1243/095440905X8790

Markine, V. L., & Shevtsov, I. Y. (2011). Optimization of a wheel profile accounting for design robustness. *Proceedings of the Institution of Mechanical Engineers, Part F: Journal of Rail and Rapid Transit*, *225*(5), 433–442. https://doi.org/10.1177/09544097JRRT305

Masselink, H. J. (2023). *Numerical Optimisation of Railway Sleepers in Transition Zones* [Doctoral dissertation, Delft Universtity of Technology].

Montgomery, D. C. (2013). *Design and analysis of experiments* (Eighth edition). John Wiley & Sons, Inc.

Sañudo, R., dell'Olio, L., Casado, J., Carrascal, I., & Diego, S. (2016). Track transitions in railways: A review. *Construction and Building Materials*, *112*, 140–157. https://doi.org/10.1016/j.conbuildmat.2016.02.084

Thomson, Q., & Martins, J. R. (2011). Adaptive accuracy trust region: Using cross-validation in the optimization process. *Engineering Optimization*, *43*(6), 615–633. https://doi.org/10.1080/0305215X.2010.508521

TU Delft. (n.d.). Railway Engineering: An Integral Approach 1.2.1 to 1.2.5. https://ocw.tudelft.nl/course-readings/2-2-1-track-systems/

Zhu, J. Y., Thompson, D. J., & Jones, C. J. (2011). On the effect of unsupported sleepers on the dynamic behaviour of a railway track. *Vehicle System Dynamics*, *49*(9), 1389–1408. https://doi.org/10.1080/00423114.2010.524303

Appendix A: Optimized Latin Hypercube samples

Table 7: Sample 1: Lengths and Widths

Sleeper	Length (m)	Width (m)
1	2.85	0.375
2	3.05	0.395
3	3.25	0.375
4	2.75	0.375
5	3.05	0.345
6	3.05	0.385
7	3.05	0.355
8	3.05	0.345
9	2.65	0.335
10	2.65	0.305
11	2.95	0.315
12	3.15	0.385
13	3.45	0.355
14	2.55	0.305
15	3.45	0.385
16	2.95	0.305
17	3.35	0.305
18	3.35	0.325
19	2.65	0.395
20	2.95	0.385
21	3.15	0.365
22	3.45	0.375
23	3.15	0.365
24	3.05	0.325
25	3.25	0.335
26	2.85	0.315
27	2.55	0.315
28	2.55	0.355
29	3.05	0.355
30	3.25	0.355
31	2.95	0.325

Table 8: Sample 2: Lengths and Widths

Sleeper	Length (m)	Width (m)
1	3.15	0.305
2	2.95	0.335
3	3.05	0.335
4	2.65	0.315
5	2.75	0.325
6	2.55	0.345
7	3.45	0.365
8	3.45	0.305
9	3.15	0.395
10	3.25	0.375
11	2.65	0.365
12	2.75	0.365
13	2.65	0.345
14	3.15	0.355
15	2.95	0.365
16	2.75	0.395
17	2.95	0.315
18	2.85	0.315
19	2.85	0.315
20	2.75	0.375
21	3.45	0.325
22	2.95	0.355
23	3.25	0.335
24	2.75	0.315
25	3.35	0.365
26	2.95	0.345
27	2.75	0.395
28	3.15	0.325
29	3.45	0.315
30	3.35	0.395
31	2.75	0.345

Table 9: Sample 3: Lengths and Widths

Sleeper	Length (m)	Width (m)
1	3.05	0.385
2	3.45	0.305
3	2.75	0.395
4	3.25	0.345
5	3.35	0.355
6	2.65	0.365
7	2.55	0.325
8	2.85	0.325
9	3.25	0.345
10	2.95	0.385
11	3.05	0.375
12	2.85	0.355
13	3.05	0.395
14	2.95	0.365
15	2.75	0.395
16	2.55	0.335
17	3.05	0.395
18	2.65	0.305
19	2.55	0.305
20	3.45	0.355
21	3.05	0.345
22	3.25	0.325
23	3.35	0.385
24	3.15	0.385
25	3.15	0.355
26	3.35	0.365
27	3.25	0.355
28	2.75	0.345
29	2.55	0.345
30	3.05	0.335
31	2.85	0.315

Table 10: Sample 4: Lengths and Widths

Sleeper	Length (m)	Width (m)
1	3.35	0.345
2	2.75	0.325
3	2.85	0.305
4	3.05	0.325
5	2.85	0.305
6	2.85	0.315
7	3.35	0.305
8	3.15	0.385
9	2.55	0.355
10	3.05	0.355
11	2.55	0.335
12	3.35	0.395
13	2.75	0.375
14	2.85	0.395
15	3.35	0.345
16	3.25	0.365
17	3.25	0.385
18	3.25	0.335
19	2.95	0.375
20	3.25	0.325
21	2.95	0.385
22	3.05	0.315
23	2.55	0.315
24	2.85	0.345
25	2.95	0.385
26	2.65	0.355
27	3.15	0.385
28	3.35	0.395
29	2.75	0.335
30	2.55	0.305
31	3.15	0.335

Table 11: Sample 5: Lengths and Widths

Sleeper	Length (m)	Width (m)
1	2.65	0.365
2	2.55	0.385
3	3.35	0.385
4	3.15	0.385
5	3.25	0.385
6	3.15	0.305
7	2.85	0.375
8	3.25	0.355
9	2.75	0.365
10	3.15	0.345
11	3.45	0.345
12	3.05	0.375
13	3.35	0.335
14	3.05	0.375
15	3.25	0.335
16	2.65	0.385
17	2.55	0.325
18	3.05	0.385
19	3.05	0.325
20	2.85	0.365
21	3.25	0.335
22	2.75	0.395
23	2.85	0.345
24	3.25	0.335
25	2.65	0.345
26	3.45	0.395
27	2.95	0.375
28	3.45	0.375
29	3.15	0.395
30	2.65	0.325
31	2.55	0.365

Table 12: Sample 6: Lengths and Widths

Sleeper	Length (m)	Width (m)
1	3.45	0.315
2	2.85	0.365
3	2.55	0.365
4	2.85	0.305
5	2.65	0.365
6	2.95	0.355
7	2.65	0.395
8	2.55	0.315
9	2.85	0.315
10	3.45	0.365
11	3.35	0.325
12	2.95	0.335
13	3.15	0.305
14	3.25	0.315
15	2.65	0.305
16	3.05	0.315
17	3.45	0.345
18	3.15	0.375
19	3.45	0.345
20	3.05	0.305
21	3.35	0.395
22	3.35	0.335
23	2.95	0.355
24	2.65	0.395
25	2.55	0.315
26	3.05	0.375
27	2.65	0.305
28	3.25	0.385
29	3.35	0.365
30	3.15	0.345
31	3.35	0.355

Table 13: Sample 7: Lengths and Widths

Sleeper	Length (m)	Width (m)
1	2.55	0.335
2	3.15	0.345
3	2.95	0.355
4	3.35	0.355
5	2.55	0.315
6	3.45	0.325
7	2.75	0.335
8	2.65	0.395
9	3.35	0.305
10	2.85	0.325
11	2.85	0.305
12	2.65	0.345
13	3.25	0.365
14	2.75	0.325
15	2.55	0.325
16	3.15	0.355
17	3.15	0.355
18	3.45	0.355
19	3.15	0.385
20	2.65	0.345
21	2.65	0.355
22	2.65	0.365
23	2.65	0.395
24	2.95	0.375
25	3.45	0.395
26	3.15	0.385
27	3.05	0.345
28	2.95	0.305
29	3.25	0.305
30	2.95	0.375
31	3.45	0.395

Table 14: Sample 8: Lengths and Widths

Sleeper	Length (m)	Width (m)
1	2.95	0.355
2	3.35	0.315
3	3.45	0.325
4	2.95	0.335
5	3.45	0.395
6	3.25	0.375
7	2.95	0.315
8	2.95	0.375
9	3.05	0.375
10	2.75	0.335
11	2.75	0.385
12	2.55	0.315
13	2.85	0.325
14	3.35	0.385
15	3.15	0.315
16	2.85	0.325
17	2.75	0.365
18	2.95	0.395
19	2.75	0.355
20	2.55	0.335
21	2.75	0.375
22	2.85	0.385
23	2.75	0.375
24	2.55	0.365
25	2.85	0.305
26	2.75	0.305
27	3.45	0.365
28	2.85	0.365
29	2.65	0.325
30	2.75	0.385
31	3.25	0.375

Table 15: Sample 9: Lengths and Widths

Sleeper	Length (m)	Width (m)
1	2.75	0.325
2	3.25	0.355
3	3.15	0.345
4	2.55	0.365
5	2.95	0.375
6	2.75	0.395
7	3.15	0.345
8	2.75	0.365
9	2.95	0.385
10	2.55	0.395
11	3.25	0.395
12	3.45	0.305
13	2.55	0.315
14	3.45	0.335
15	2.85	0.355
16	3.45	0.375
17	2.65	0.375
18	2.55	0.365
19	3.35	0.365
20	3.35	0.395
21	2.85	0.315
22	3.15	0.345
23	3.05	0.305
24	3.45	0.305
25	2.75	0.375
26	2.55	0.335
27	3.35	0.335
28	3.05	0.335
29	2.85	0.385
30	2.85	0.315
31	3.05	0.305

Table 16: Sample 10: Lengths and Widths

Sleeper	Length (m)	Width (m)
1	3.25	0.395
2	2.65	0.375
3	2.65	0.315
4	3.45	0.395
5	3.15	0.335
6	3.35	0.335
7	3.25	0.385
8	3.35	0.335
9	3.45	0.325
10	3.35	0.315
11	3.15	0.355
12	3.25	0.325
13	2.95	0.385
14	2.65	0.345
15	3.05	0.375
16	3.35	0.345
17	2.85	0.335
18	2.75	0.345
19	3.25	0.335
20	3.15	0.315
21	2.55	0.305
22	2.55	0.305
23	3.45	0.325
24	3.35	0.355
25	3.05	0.325
26	3.25	0.325
27	2.85	0.325
28	2.65	0.315
29	2.95	0.375
30	3.45	0.365
31	2.65	0.385